NASA Technical Memorandum 82759

Interaction of Upstream Flow Distortions With High Mach Number Cascades

Gerald W. Englert
Lewis Research Center
Cleveland, Ohio

Prepared for the
Twenty-seventh Annual International Gas Turbine Conference
sponsored by the American Society of Mechanical Engineers
London, England, April 18-22, 1982

NASA

INTERACTION OF UPSTREAM FLOW DISTORTIONS WITH HIGH MACH NUMBER CASCADES

by Gerald W. Englert*
National Aeronautics and Space Administration
Lewis Research Center
Cleveland, Ohio 44135

E-1078

NOMENCLATURE[1]

A,a	distortion amplitudes in x and y directions of Fig. 1
$\mathscr{A},\mathscr{B},C$	distortion amplitudes in $\hat{I},\hat{J},\hat{K}$ directions of Fig. 1
$a_n^{\pm}$	combination of terms defined by (32)
B	coefficients in (58)
b	constant in a convergence producing term of $\kappa_d^{\pm}(\alpha)$
$b_{i,j}$	coefficients in description of subsonic vortical flow in (19)
c	chord
d	mean circumferential distance between blades, Fig. 1
$c_u^{\dagger},c_d^{\dagger}$	combination of terms defined by (48) and (68) respectively
f	arbitrary function
h	blade height
I	integrand of (54)
$\hat{I},\hat{J},\hat{K}$	unit orthogonal vectors in upstream distortion coordinate system
i	$(-1)^{1/2}$
K_u,K_d	branch points in α space
$K_{m,n}$	combination of terms defined by (23)
$\mathscr{K}_{\bar{m}}$	combination of terms defined by (24)
k_u,k_d	wave numbers $= M_u\omega_u/\beta_u^2$ and $M_d\omega_d/\beta_d^2$ respectively
k_q	spanwise wave number $= \pi q/h$
L	mean circumferential distance along blade row
$\mathscr{L}$	lift
M	Mach number
$\mathscr{M}$	moment
N	integral number of distortion transverse wave lengths in distance $s^{\dagger}$ along x
P_u,P_d	amplitudes of p_u,p_d
p_u,p_d	pressure perturbation non-dimensionalized by $\rho_u\mathscr{U}_u^2$
p,q	Fourier indices in (1)
$Q^{\pm}$	combination of terms used in (10b)
R	combination of terms used in (30)
S	solidity = chord/blade gap = 1/dimensionless d
s	interblade distance along y in Fig. 1
$s^{\dagger}$	$(\sin\chi)/S$ as in Fig. 1
t	time non-dimensionalized by multiplying by $\mathscr{U}_u/c$
t_1,t_2	combinations of terms defined by (33) and (34)
$\mathscr{U}$	mean velocity
$\hat{U},\hat{V},\hat{W}$	amplitudes of $\hat{u},\hat{v},\hat{w}$
$\hat{u},\hat{v},\hat{w}$	total, vortical, and acoustic velocity perturbations non-dimensionalized by $\mathscr{U}_u$
x,y,z	blade coordinates (Fig. 1) non-dimensionalized by blade chord
$\tilde{x}_u,\tilde{x}_d$	$x + s^{\dagger}$ and $x + s^{\dagger} - 1$ respectively
Y_1,Y_2,Y_3	orthogonal coordinates in a fixed frame upstream of cascade
α	Fourier transform variable
$\alpha_n^{\pm}$	combination of terms defined by (69)
β_u,β_d	$\left(M_u^2 - 1\right)^{1/2}$ and $\left(1 - M_d^2\right)^{1/2}$ respectively

---

*Aerospace Research Engineer.

[1]The velocity and pressure perturbations downstream of the shock are the differences between actual and mean downstream values, however they are non-dimensionalized by the upstream quantities $\mathscr{U}_u$ and $\rho\mathscr{U}_u^2$ as discussed on pg. 574 of [2].

$r_n^{(u)}, r_n^{(d)}$ combination of terms defined by (50) and (67) respectively

γ ratio of specific heats of an ideal gas

γ_u, γ_d $\left(\alpha^2 - k_u^2 - k_q^2/\beta_u^2\right)^{1/2}$ and $\left(\alpha^2 - k_d^2 + k_q^2/\beta_d^2\right)^{1/2}$ respectively

Δ_u, Δ_d combination of terms defined by (41) and (56) respectively

δ imaginary part of integration contour for Φ_u

δ_j^i Kronecker delta; = 0 if $i \neq j$; = 1 if $i = j$

ϵ_u, ϵ_d small damping terms in γ_u and γ_d respectively

$\eta_n^{\pm}$ combination of terms defined by (52)

θ arbitrary variable illustrating periodicity relation

κ_u, κ_d variables defined by (43) and (60) respectively

Λ_u, Λ_d combinations of terms defined by (40) and (55)

$\lambda_n^{(u)}, \lambda_n^{(d)}$ combinations of terms defined by (12) and (53)

μ angle between upstream and blade coordinate systems of Fig. 1

ν direction of transport of upstream distortion with respect to axis of turbomachine

$\nu_n^{\pm}$ combination of variables defined by (49)

ρ density

σ interblade phase angle defined by (3)

Φ amplitude of φ

φ velocity potential

χ stagger angle = $\nu - \mu$

Ψ_u, Ψ_d $\left(\omega_u^2 + k_q^2\right)^{1/2}$ and $\left(\omega_d^2 + k_q^2\right)^{1/2}$ respectively

ψ_u, ψ_d $\left(k_u^2 + k_q^2/\beta_u^2\right)^{1/2}$ and $\left(k_d^2 - k_q^2/\beta_d^2\right)^{1/2}$ respectively

Ω arbitrary function in (13)

ω frequency = $2\pi p \mathcal{U}_b/L$ in dimensional form

ω_u, ω_d reduced frequencies $\omega c/\mathcal{U}_u$ and $\omega c/\mathcal{U}_d$ respectively

SUBSCRIPTS:

b blade

d,u downstream and upstream of shock respectively

n integer

p,q Fourier indices describing upstream distortion

s shock

1,2,3 correspond to $\hat{I},\hat{J},\hat{K}$ and to x,y,z directions in upstream distortion and in blade coordinate systems of Fig. 1 respectively

SUPERSCRIPTS:

d,u downstream and upstream of shock respectively

+,- upper and lower half planes of α space

~ implies both vortical and acoustic properties

→ vector

^ unit vector

INTRODUCTION

Associated with high performance axial fans and compressors of aircraft engines are slender blades with high tip Mach numbers [1]. Such blade rows may be vulnerable to distortion of the oncoming airstream such as atmospheric gusts, wakes from upstream struts and guide vanes, and maldistributions in air inlets and ducts; all of which tend to force the blades into vibratory motions. Of concern is the influence of strong shocks occurring in blade passages. When such shocks couple to the distortion pattern they can have an oscillatory influence on the blade pressure distributions, forces, and moments. The influence of the blade row on the distortion is also of importance since it passes on to influence other components of the propulsion system.

The recent linearized theory of Goldstein, Braun, and Adamczyk [2], which analyzes unsteady flow in supersonic cascades with strong in-passage shocks, is applied to the distortion problem in the investigation reported herein. The flutter boundary conditions of [2] are however replaced with those of the three-dimensional distortion of Goldstein [3]. This disturbance profile (Fig. 1) has components parallel to, and in two directions transverse to, a mean flow velocity $\mathcal{U}$. Relative to the cascade the mean velocity, $\mathcal{U}_u$, is supersonic in this study. The component of $\mathcal{U}_u$ parallel to the axis of the turbomachine is, however, subsonic. The Mach waves from the leading edges of the blades then extend forward of the edge of each successive blade permitting interaction between blades through the supersonic, as well as the subsonic, flow media. This is usually the case of interest in advance type fans and compressors.

The cascade (Fig. 1) is envisioned as an "unrolled annulus" which translates with a blade velocity $\mathcal{U}_b$. Integral multiples of distortion wave length must however equal a mean circumferential distance along the face of the blade row. Spanwise flow distributions are considered at limited blade aspect ratios although centrifugal and Coriolis forces are neglected. Within the confines of linearized theory blade thickness, camber, and angle of attack make no contribution to the unsteady forces (Chap. 3 of [3]). Such time independent effects can therefore be superposed on the results of this study in which the blades take the form of flat parallel plates.

Separation of the flow into two distinct (sub- and supersonic) regions permits solution of the potential part of the flow field in each one by adaptation of the Wiener Hopf technique [2]. In the first region a supersonic flow extends from upstream infinity to a cascade which extends to downstream infinity. In the second region a subsonic flow is guided by parallel blade passages from upstream infinity, past the trailing edges, and on to downstream infinity. The supersonic solution is independent of downstream influence and the subsonic solution is kept sufficiently arbitrary to satisfy shock boundary conditions. Matching of solutions at the shock interface involves inversion of a large nearly diagonal matrix. This is easily done numerically.

In the present effort the shock is assumed to be located an arbitrarily small distance inside the leading edge of the blade so that it doesn't disturb the supersonic flow on the upper surface in this region.

FORMULATION

By the splitting theorem (chap. 5 of [3]) any linearized description of an inviscid compressible fluid can be decomposed into two non-interacting motions; one of which is vortical and the other acoustic in nature. The vortical motion is solenoidal, and its substantial derivative is equal to zero. Shear layers, for example, are vortical in nature, and are an effective means of forming flow distortions. The acoustic motion, on the other hand, is irrotational and has a velocity potential which satisfies the convected wave equation.

Vortical Motion Upstream of Shock

The upstream flow distortion of interest herein is vortical. Its velocity (Fig. 1) is specified by the double Fourier series (char. 5 of [3])

$$\hat{v} = \sum_{p,q} [(\hat{I}\mathscr{A}_{pq} + \hat{J}\mathscr{B}_{pq}) \cos(\pi q Y_3/h) + \hat{K}C_{pq} \sin(\pi q Y_3/h)] e^{i2\pi p Y_2/L \cos\nu} \quad (1)$$

For each set of Fourier indices the distortion amplitudes are $\mathscr{A}_{pq}$, $\mathscr{B}_{pq}$, and C_{pq}, for motion in the three orthogonal directions $\hat{I}$, $\hat{J}$, and $\hat{K}$. As in [3] there is an integral number, p, of distortion wave lengths parallel to the face of the blade row where L is a mean circumferential distance. The spanwise wave length is the hub-to-shroud distance, h, divided by Fourier index q. Distance and velocity are non-dimensionalized by blade chord and mean upstream velocity, $\mathscr{U}_U$ of Fig. 1, respectively.

Transformation of (1) to blade coordinates (x,y,z) moving with velocity $\mathscr{U}_b$ relative to $\mathscr{U}$ gives the vortical motion a harmonic time dependence. In this system

$$\hat{v}_U = a\, e^{-i\omega_U t} \cos(k_q z)\bar{V}_U \quad (2a)$$

where time has been non-dimensionalized by $\mathscr{U}_U/c$ and where

$$\bar{V}_U = \begin{bmatrix} V_1^{(u)} \\ V_2^{(u)} \\ V_3^{(u)} \end{bmatrix} = e^{i\omega_U(x+s^\dagger+y\cot\mu)} \begin{bmatrix} A/a \\ 1 \\ \tan(k_q z)C/a \end{bmatrix}, \quad (2b)$$

and spanwise wave number, k_q, is equal to $\pi a/h$. The exponent in (2b) sets the interblade phase angle, σ, as

$$\sigma = \omega_U(s^\dagger + s\cot\mu). \quad (3)$$

The x and t dependence in (2a) and (2b) together satisfy the condition that the substantial derivative, $D\hat{v}_U/Dt$, is equal to zero. The components of the distortion amplitudes in the x,y,z directions are now

$$a = -\mathscr{A}_{pq}\sin\mu + \mathscr{B}_{pq}\cos\mu, \quad (4a)$$

$$A = \mathscr{A}_{pq}\cos\mu + \mathscr{B}_{pq}\sin\mu, \quad (4b)$$

and, by the solenoidal condition on $\hat{v}_U$,

$$C = -2i\pi h\mathscr{B}/qL\cos\nu = -\frac{2i\pi p}{k_q L\cos\nu}(a\cos\mu + A\sin\mu). \quad (4c)$$

Since final results can be superposed, only one set of Fourier components will be carried through the analysis; thus the p and q indices will normally be omitted from the flow variables.

Acoustic Motion Upstream of Shock

The total motion, $\hat{u}_U = \hat{v}_U + \hat{w}_U$, will satisfy the inviscid tangency condition at the blade surface if the normal component of the acoustic (potential) motion satisfies

$$w_2^{(u)} = \frac{\partial\varphi_U}{\partial y} = -a\cos(k_q z)e^{i\omega_U(x+s^\dagger+ns\cot\mu-t)} \quad (5)$$

for $-s^\dagger < x - ns^\dagger < 0$, $0 < z < h$, and $n = 0, \pm1, \pm2, \cdots$. By inspection, the solution to the linearized convected wave equation,

$$(\nabla^2 - D^2/Dt^2)\varphi_U = 0 \quad (6)$$

which satisfys (5) is of the form

$$\varphi_U = -a\cos(k_q z)e^{-i\omega_U t}\Phi_U(x,y) \quad (7)$$

Thus

$$\hat{w}_U = a\, e^{-i\omega_U t}\cos(k_q z)\bar{W}_U \quad (8a)$$

where

$$\bar{W}_U = \begin{bmatrix} -a\Phi_U/ax \\ -a\Phi_U/ay \\ k_q\tan(k_q z)\Phi_U \end{bmatrix} \quad (8b)$$

Note that the z components of both Eqs. (2) and (8) individually satisfy the flow tangency condition at both the hub and shroud.

Pressure, p_U, is associated with the acoustic motion, satisfies the wave equation, and can also be expressed in the form

$$p_U = -a\, e^{-i\omega_U t}\cos(k_q z)P_U(x,y) \quad (9a)$$

where

$$P_U = \left(i\omega_U - \frac{\partial}{\partial x}\right)\Phi_U \quad (9b)$$

The procedure for solution of $\phi_u(x,y)$ by use of the Wiener-Hopf technique is given in Appendix 1. The results for $0 \le y \le s$ are

$$\phi_u(x,y) =$$

$$-is\,\kappa_u^-\left(\frac{k_u}{M_u}\right)\sum_{n=-\infty}^{\infty}\frac{e^{-i\left[\left(\nu_n^+ - M_u k_u\right)\tilde{x}_u + \frac{y}{s}\left(d_u^+\Gamma_n^{(u)} - \nu_n^+ s^+\right)\right]}}{\left(\nu_n^+ - \frac{k_u}{M_u}\right)\left[\kappa_u^-\left(\nu_n^+\right)\right]'\left(d_u^+\Gamma_n^{(u)} - \nu_n^+ s^+\right)}$$

$$\text{for } x \le -\beta_u(s-y) \qquad (10a)$$

where

$$\left[\kappa_u^-\left(\nu_n^+\right)\right]' \equiv d\kappa_u^-\left(\nu_n^+\right)\Big/ d\nu_n^+,$$

and

$$\phi_u(x,y)$$

$$= -e^{i\omega_u\tilde{x}_u}\left\{\frac{\cosh\left[\Psi_u(y-s)\right] - e^{i(\sigma-\omega_u s^+)}\cosh\left(\Psi_u y\right)}{\Psi_u \sinh\left(\Psi_u s\right)}\right\}$$

$$+\sum_{n=-\infty}^{\infty}\cos\left(\frac{n\pi y}{s}\right)\left[\frac{e^{i\left(M_u k_u - \lambda_n^{(u)}\right)x}\,Q_n^+}{\frac{k_u}{M_u} - \lambda_n^{(u)}} + \frac{e^{i\left(M_u k_u + \lambda_n^{(u)}\right)x}\,Q_n^-}{\frac{k_u}{M_u} + \lambda_n^{(u)}}\right]$$

$$\text{for } x > -\beta_u(s-y) \qquad (10b)$$

where

$$Q_n^{\pm} = \frac{e^{i(\sigma-n\pi)} - e^{i\left(M_u k_u \mp \lambda_n^{(u)}\right)s^+}}{\pm\lambda_n^{(u)}\beta_u^2 s\left(1+\delta_n^0\right)}\,\frac{\kappa_u^-\left(k_u/M_u\right)}{\kappa_u^-\left(\pm\lambda_n^{(u)}\right)}, \qquad (11)$$

$$\lambda_n^{(u)} = \left[\left(\frac{n\pi}{s}\right)^2 + k_u^2 + \left(\frac{k_a}{\beta_u}\right)^2\right]^{1/2}, \text{ and } \Psi_u = \left(\omega_u^2 + k_a^2\right)^{1/2}. \qquad (12)$$

Substitution of (10) into (8) and (9) determines the velocity of the acoustic motion and the pressure in the supersonic region ahead of the shock.

Vortical Motion Downstream of Shock

In this region let the velocity, v_d, take the form

$$\hat{v}_d = a\cos\left(k_a z\right)e^{i(\omega_d x - \omega_u t)}\,\hat{\Omega}(y) \qquad (13)$$

which satisfies the spanwise wall tangency condition and has a substantial derivative equal to zero. To satisfy periodicity let

$$e^{i\omega_d(x+ns^+)}\,\hat{\Omega}(y+ns) = e^{in\sigma}\,e^{i\omega_d x}\,\hat{\Omega}(y) \qquad (14)$$

for blade number $n = 0, \pm1, \pm2, \cdots$. The solenoidal condition will be invoked later, completing the splitting theorem requirements for $\hat{v}_d$ to be vortical.

It is anticipated that a part, $\tilde{\hat{v}}_d$, of $\hat{v}_d$ can be found which is both vortical and acoustic, as in Eq. (5.12) of [3]. Combining $\tilde{\hat{v}}_d$ with the potential flow, $\hat{w}_d$, may then simplify determination of the remaining part of $\hat{v}_d$. Such a procedure is used to advantage in [2]. Associated with $\tilde{\hat{v}}_d$ is a potential $\tilde{\hat{\varphi}}_d$ such that $\nabla\tilde{\hat{\varphi}}_d = \tilde{\hat{v}}_d$, and since $\nabla\cdot\tilde{\hat{v}}_d = 0$ it follows that $\nabla^2\tilde{\hat{\varphi}}_d = 0$. Since $\tilde{\hat{v}}_d$ is vortical, $\tilde{\hat{\varphi}}_d$ makes no contribution to the pressure distribution. Let $\tilde{\hat{\varphi}}_d$ take the form of (13)

$$\tilde{\hat{\varphi}}_d = a\cos\left(k_a z\right)e^{i(\omega_d x - \omega_u t)}\,f(y) \qquad (15)$$

For $\tilde{\hat{\varphi}}_d$ to satisfy Laplace's equation, f must satisfy

$$-\left(\omega_d^2 + k_a^2\right)f + f'' = 0. \qquad (16)$$

A solution of (16) which enables $\tilde{\hat{\varphi}}_d$ to satisfy periodicity as well as to cancel the normal component of $\hat{v}_d$ at the blade surfaces is,

$$f = \frac{\Omega_2(ns)}{\Psi_d \sinh\left(\Psi_d s\right)}\left\{\cosh(\Psi_d s)\cosh\left[\Psi_d(y-ns)\right] - \cosh\left[\Psi_d(y-ns-s)\right]\right\} \qquad (17)$$

where $\Psi_d \equiv \sqrt{\omega_d^2 + k_a^2}$. The subscripts 1,2,3 on Ω identify the components of $\hat{\Omega}$ in the x, y, and z directions respectively.

Substitution of (13), (15), and (17) into the identity

$$\hat{v}_d \equiv \left(\hat{v}_d - \nabla\tilde{\hat{\varphi}}_d\right) + \nabla\tilde{\hat{\varphi}}_d \qquad (18)$$

shows that the first term $\left(\hat{v}_d - \nabla\tilde{\hat{\varphi}}_d\right)$ makes no contribution to the blade boundary conditions (since its y component vanishes at $y = 0$ and s) although it does contribute to the matching of flows at the shock boundary. With sufficient generality the strictly vortical part of (18) can thus be sufficiently described by Fourier sine and cosine series as

$$\hat{v}_d(x,y,z) =$$

$$a \cos(k_q z) e^{i(\omega_d x - \omega_u t)} \begin{bmatrix} \sum_{m=1}^{\infty} b_{1,m} \cos(m\pi y/s) \\ i \sum_{m=1}^{\infty} b_{2,m} \sin(m\pi y/s) \\ -k_q \tan(k_q z) \sum_{m=1}^{\infty} b_{3,m} \cos(m\pi y/s) \end{bmatrix} \tag{19}$$

and the $\nabla\tilde{\varphi}_d$ part of (18) will be included in $w_d = \nabla\varphi_d$. This procedure is close to that of [2] which utilizes a stream function for a two-dimensional vortical motion.

The solenoidal condition has already been invoked in $\hat{v}_d$. Using it in (19) for $\hat{v}_0$ gives

$$\omega_d b_{1,m} + \frac{m\pi}{s} b_{2,m} + ik_q^2 b_{3,m} = 0. \tag{20}$$

Acoustic Motion Downstream of Shock

The acoustic field downstream of the shock is composed of two parts. An infinite "duct" solution, to the convected wave equation, having downstream running waves accounts for shock boundary conditions. A "cascade" solution, on the other hand, gives the upstream (or reflected) waves. Each solution, as well as the vortical motion of the preceding section, individually satisfies the wall tangency condition. The sum of the two acoustic solutions must satisfy the Kutta condition. In both solutions the velocity potential, φ_d, again takes the form

$$\varphi_d(x,y,z) = a \cos(k_q z) e^{-i\omega_u t} \Phi_d(x,y) \tag{21}$$

The procedure to obtain the combined potential $\Phi_d = \Phi_d^{duct} + \Phi_d^{cascade}$ is given in Appendix II. The results for $0 \le y \le s$ are

$$\Phi_d(x,y) =$$

$$\frac{1}{\tau} \sum_{n=0}^{\infty} \left[\frac{B_n e^{i n_n^+ x}}{\frac{k_d}{M_d} - \lambda_n^{(d)}} + \sum_{m=0}^{\infty} B_m K_{mn} \frac{e^{i n_n^- \tilde{x}_d}}{\lambda_n^{(d)} + \frac{k_d}{M_d}} \right] \cos \frac{n\pi y}{s}$$

$$\text{for } 0 \le x < 1 - s^\dagger \tag{22a}$$

$$\Phi_d(x,y) = \frac{1}{\tau} \sum_{n=0}^{\infty} B_n \left[\frac{\cos\left(\frac{n\pi y}{s}\right) e^{i\left[n_n^+(x-s^\dagger)+\sigma-n\pi\right]}}{\left(\frac{k_d}{M_d} - \lambda_n^{(d)}\right)\left[e^{-i\left(n_n^+ s^\dagger - \sigma + n\pi\right)} - 1\right]} + \frac{e^{i n_n^+}}{2} \left[e^{i(n\pi - \sigma)} - e^{-i n_n^+ s^\dagger} \right] \right.$$

$$\left. \times \left\{ \frac{\kappa_d^-\left(-\lambda_n^{(d)}\right) \cosh\left[\Psi_d(y-s)\right] e^{i\omega_d \tilde{x}_d}}{\left(\lambda_n^{(d)} - \frac{k_d}{M_d}\right) \kappa_d^-\left(-\frac{k_d}{M_d}\right)\left[\cosh(\Psi_d s) - \cos(\sigma - \omega_d s^\dagger)\right]} + \sum_{m=-\infty}^{\infty} \frac{\cos\left[\left(1 - \frac{y}{s}\right)\left(\sigma_c^\dagger r_m^{(c)} - s^\dagger \alpha_m^-\right)\right] \chi_m^-\left(\lambda_n^{(c)}\right)}{\left(\alpha_m^- + \frac{k_c}{M_c}\right) e^{i\left(\alpha_m^- + M_c k_c\right)\tilde{x}_c}} \right\} \right]$$

$$+ \frac{1}{\tau} \sum_{n=0}^{\infty} \sum_{m=0}^{\infty} B_m K_{m,n} \frac{e^{i\left[n_n^-\left(\tilde{x}_c - s^\dagger\right) + \sigma + n\pi\right]} \cos\left(\frac{n\pi y}{s}\right)}{\left[e^{i\left(\sigma - n_n^- s^\dagger + n\pi\right)} - 1\right]\left(\lambda_n^{(d)} + \frac{k_d}{M_d}\right)} \qquad \text{for } 1 - s^\dagger < x < 1 \tag{22b}$$

and

$$\phi_d(x,y) = \frac{1}{i}\sum_{n=0}^{\infty} B_n \frac{e^{in_n^+}}{2}\left[e^{i(n\pi-\sigma)} - e^{-in_n^+ s^+}\right]\left\{\frac{\kappa_d^-\left(-\lambda_n^{(d)}\right)\left[\cosh\left(\nu_d(y-s)\right) - \cosh\left(\nu_d y\right)e^{i(\sigma-\omega_d s^+)}\right]}{\left(\lambda_n^{(d)} - \frac{k_d}{M_d}\right)\kappa_d^-\left(-\frac{k_d}{M_d}\right)\left[\cosh\left(\nu_d s\right) - \cos\left(\sigma - \omega_d s^+\right)\right]} e^{i\omega_d \tilde{x}}\right.$$

$$\left. + \sum_{m=-\infty}^{\infty} \frac{\cos\left[\left(1-\frac{y}{s}\right)\left(d_d^+ r_m^{(d)} - s^+\alpha_m^-\right)\right] - \cos\left[\frac{y}{s}\left(d_d^+ r_m^{(d)} - s^+\alpha_m^-\right)\right]e^{i\left[\sigma^+\left(\alpha_m^- + M_d k_d\right)s^+\right]}}{\left(\alpha_m^- + \frac{k_d}{M_d}\right)e^{i\left(\alpha_m^- + M_d k_d\right)\tilde{x}_d}} \mathcal{I}_m^-\left(\lambda_n^{(d)}\right)\right\} \quad \text{for } 1 \le x. \qquad (22c)$$

where

$$K_{m,n} \equiv \frac{e^{in_m^+}}{2\left(1+\varepsilon_n^0\right)}\left[e^{i(m\pi-\sigma)} - e^{-in_m^- s^+}\right]\left[e^{i\left(\sigma - n_m^- s^+ + n\pi\right)} - 1\right] \times \frac{\kappa_c^-\left(-\lambda_m^{(d)}\right)\left(\lambda_n^{(d)} + \frac{k_d}{M_d}\right)}{\kappa_d^+\left(\lambda_n^{(d)}\right)\left(\lambda_n^{(d)} + \lambda_m^{(d)}\right)\beta_d^2 s\lambda_m^{(d)}}, \qquad (23)$$

$$\mathcal{I}_m^-\left(\lambda_n^{(d)}\right) \equiv \frac{\kappa_d^-\left(-\lambda_n^{(d)}\right)\left(d_d^+ r_m^{(d)} - \alpha_m^- s^+\right)}{\kappa_c^-\left(\alpha_m^-\right)d_c^+\left(s^+ r_m^{(c)} - \alpha_m^- d_c^+\right)\left(\alpha_m^- + \lambda_n^{(c)}\right)\sin\left(\alpha_m^- s^+ - d_c^+ r_m^{(c)}\right)}, \qquad (24)$$

$\nu_g \equiv \sqrt{\omega_c^2 + k_a^2}$, and ε_n^0 is the Kronecker delta. Determination of the coefficients B_m of (22) and $b_{j,n}$ ($j = 1,2,3$) of (19) and (20) is made possible with the additional information supplied by the following three shock relations.

Relations Across Shock

The mean flow satisfies the Rankine-Hugoniot relations. Shock curvature and displacement are treated as perturbations as in [8]. The downstream vorticity, longitudinal velocity, and pressure are related to the upstream vorticity, longitudinal velocity, and pressure by the following three equations:

$$v_1^{(d)} = -\frac{M_u^2 + 1}{2M_u^2} p_d + v_1^{(u)} + \frac{1}{2}\left[M_u^2 + 1 - \frac{\gamma - 1}{\gamma + 1}\frac{\beta_u^4}{M_u^2}\right] p_u, \qquad (25)$$

$$\frac{\partial}{\partial y}\left[p_d - \left(M_u^2 + \frac{\gamma-1}{\gamma+1}\beta_u^2\right)p_u\right] = (\gamma+1)\frac{M_u^2 M_d^2}{\beta_u^2\beta_d^2} \times \left[\left(\frac{\partial v_2^{(d)}}{\partial x} - \frac{\partial v_1^{(d)}}{\partial y}\right) - \frac{u_u}{u_d}\left(\frac{\partial v_2^{(u)}}{\partial x} - \frac{\partial v_1^{(u)}}{\partial y}\right)\right], \qquad (26)$$

and

$$\frac{\partial}{\partial z}\left[p_d - \left(M_u^2 + \frac{\gamma-1}{\gamma+1}\beta_u^2\right)p_u\right] = (\gamma+1)\frac{M_u^2 M_d^2}{\beta_u^2\beta_d^2} \times \left[\left(\frac{\partial v_3^{(d)}}{\partial x} - \frac{\partial v_1^{(d)}}{\partial z}\right) - \frac{u_u}{u_d}\left(\frac{\partial v_3^{(u)}}{\partial x} - \frac{\partial v_1^{(u)}}{\partial z}\right)\right], \qquad (27)$$

These equations differ from those of [2] by addition of an upstream vorticity and a spanwise distribution of pressure and velocity.

Matching of Solutions at Shock Boundary

Equation (26) can easily be combined with (27) to yield

$$\frac{\partial}{\partial y}\left(\frac{u_u}{u_d} v_3^{(u)} - v_3^{(d)}\right) = k_a \tan\left(k_a z\right)\left(v_2^{(d)} - v_2^{(u)}\right) \qquad (28)$$

since the z dependence enters only through $\cos(k_a z)$. Combining (28) with (2), (19), and solenoidal condition (20), and utilizing orthogonality relations between sine terms, permits determination of $b_{1,n}$ and $b_{3,n}$ in terms of $b_{2,n}$ and known quantities. The downstream vortical velocity of (19) can now be expressed as

$$\tilde{v}_d(x,y,z) = a \cos(k_q z) e^{i(\omega_u t + \omega_d x)}$$

$$\times \left[\begin{array}{l} - \sum_{m=1}^{\infty} \left[\frac{1 + (k_q s/m\pi)^2}{\omega_d s/m\pi} b_{2,m} + \frac{2isR_m (k_q/\pi\omega_u)^2}{m \exp(i\omega_d x)} \right] \cos\left(\frac{m\pi y}{s}\right) \\ \\ i \sum_{m=1}^{\infty} b_{2,m} \sin(m\pi y/s) \\ \\ -k_q \tan(k_q z) \sum_{m=1}^{\infty} \left[\frac{s b_{2,m}}{im\pi} + \frac{2sR_m}{m^2 \omega_d \exp(i\omega_d x)} \right] \cos\left(\frac{m\pi y}{s}\right) \end{array} \right] \tag{29}$$

where

$$R_m \equiv \omega_u e^{i\omega_u s^+}$$

$$\times \left[1 + i \frac{M_u}{M_d} \omega_u (\cot \mu) \frac{C}{a} \right] \frac{m \left[1 - (-1)^m \exp(i\omega_u s \operatorname{ctn} \mu) \right]}{m^2 - (\omega_u s \operatorname{ctn} \mu/\pi)^2}$$

$$\text{for } m \geq 1 = 0$$

$$= 0 \qquad \text{for } m = 0. \tag{30}$$

Use of (2), (7), (9), (10b), (21), (22a), and (29) for velocities and pressures in shock relations (25) and (26) and utilizing (377), (378), (488), (489) and (592) of [9] gives the following equation for B_n in implicit form.

$$\left[a_n^+ - \delta_0^n \frac{k_q^2 \left(2M_u^2 M_d^2 - M_u^2 - M_d^2 \right)}{\beta_d^4 M_u^2} \right] B_n$$

$$+ \left[a_n^- - \delta_0^n \frac{k_q^2 \left(2M_u^2 M_d^2 - M_u^2 - M_d^2 \right)}{\beta_d^4 M_u^2} \right] e^{-i n_n^- (1 - s^+)} \sum_{m=0}^{\infty} B_m K_{m,n}$$

$$= -i \left[\frac{2M_d^2}{\beta_d^4} \left\{ \left[\left(\frac{n\pi}{s}\right)^2 + \omega_d^2 + k_q^2 \right] \left[\frac{k_u M_u - \lambda_n^{(u)}}{k_u/M_u - \lambda_n^{(u)}} Q_n^+ \right. \right. \right.$$

$$\left. + \frac{k_u M_u - \lambda_n^{(u)}}{k_u/M_u + \lambda_n^{(u)}} Q_n^- - \frac{1}{2} \left(M_u^2 + 1 - \frac{\gamma - 1}{\gamma + 1} \frac{\beta_u^4}{M_u^2} \right) Q_n^+ + \frac{t_{2,n} - t_{1,n}}{1 + \delta_n^0} \right]$$

$$\left. + \left(1 - \delta_n^0\right) \left(\cot \mu - \frac{M_u}{M_u} \frac{a}{A} \right) \left[\left(\frac{n\pi}{s}\right)^2 + k_q^2 \right] t_{1,n}/\cot \mu \right\}$$

$$+ \frac{2\left(1 - \delta_n^0\right)}{\gamma + 1} \left(\frac{\beta_u}{\beta_d M_u} \right)^2 \left[\left(\frac{n\pi}{s}\right)^2 + k_q^2 \right] \left(M_u^2 + \frac{\gamma - 1}{\gamma + 1} \beta_u^2 \right)$$

$$\times \left(Q_n^+ + Q_n^- \right) - i \left(1 - \delta_n^0\right) \left(\frac{2k_q M_d}{\pi} \right)^2 \frac{sR_m}{n\beta_d^4} \Bigg] \tag{31}$$

where

$$a_n^{\pm} \equiv \left(\lambda_n^{(d)}\right)^2 \pm 2M_d k_d \lambda_n^{(d)} + (k_d/M_u)^2 \tag{32}$$

$$t_1 \equiv \frac{2\omega_u A}{sa} \cot \mu \, e^{i\omega_u s^+} \frac{\left[e^{i(n\pi + \omega_u s \cot \mu} - 1 \right]}{\left(\frac{n\pi}{s}\right)^2 - (\omega_u \cot \mu)^2} \tag{33}$$

$$t_2 \equiv \frac{2\omega_u}{s} e^{i\omega_u s^+} \frac{\left[e^{i(\sigma - \omega_u s^+ + n\pi)} - 1 \right]}{\left(\frac{n\pi}{s}\right)^2 + \omega_u^2 + k_q^2} \tag{34}$$

The left side of (31) reduces to (3.33) of [2] as $k_q \to 0$. The right side of (31) however replaces the flutter terms of [2] for this distortion problem. Solution of (31) for B_n is by inversion of an infinite matrix. The off-diagonal elements of this matrix came from the second term of (31) which represents acoustic waves reflected from the back end of the cascade. These are rapidly decaying waves for $(n\pi/\beta_d s)^2 + (k_q/\beta_d)^2 > k_d^2 = M_d^2 \omega_d^2/\beta_d^4$ so that, in practice, (31) can be approximated by a nearly diagonal matrix. This can be further truncated to a reasonably small number of terms. Numerical results suggest that as few as ten terms along the diagonal may, at times, give satisfactory results at values of reduced frequency less than one. Once the B_n are known the coefficient $b_{2,n}$ in the Fourier series of (29) can be obtained from shock relation (26) as

$$b_{2,n} = \frac{n\pi}{s} \omega_d \left\{ B_n + e^{-i n_n^- (1 - s^+)} \sum_{m=0}^{\infty} B_m K_{m,n} - \right.$$

$$i \left[\left(M_u^2 + \frac{\gamma - 1}{\gamma + 1} \beta_u^2 \right) \left(Q_n^+ + Q_n^- \right) + \frac{2(\gamma + 1)s}{n} \left(\frac{k_q}{\pi \omega_d} \right)^2 \left(\frac{M_u M_d}{\beta_u \beta_d} \right)^2 R_n \right.$$

$$\left. \left. + \frac{(\gamma + 1) t_1}{\cot \mu} \left(\frac{M_u M_d}{\beta_u \beta_d} \right)^2 \left(\cot \mu - \frac{a}{A} \frac{M_u}{M_d} \right) \right] \right\}$$

$$+ (\gamma + 1) \left(\frac{M_u M_d}{\beta_u \beta_d} \right)^2 \left[\omega_d^2 + \left(\frac{n\pi}{s}\right)^2 + k_q^2 \right]. \tag{35}$$

Use of (35) in (29) determines the subsonic vortical velocity for $0 < y < s$ and $x > 0$ whereas use of partial derivatives of (22) in (21) determines the corresponding acoustic velocity components. Use

of (10) in (8) along with (2) and (4) gives the acoustic and vortical velocities for $0 \leq y \leq s$ and $x < 0$. Pressure can be obtained by use of (9) and its subsonic counterpart $p_d = a\, e^{-i\omega_u t} \cos(k_q z)(i\omega_d - a/ax)\phi_d$. Extension of equations to other blades and channels is simply by use of the periodicity condition $e_n(x + ns^\dagger, ns + y) = e^{inc}\, e_0(x,y)$ where e can be any of the physical variables ϕ_u, V_u, P_u, ϕ_d, V_d, and P_d as in [2].

RESULTS

Variables which may be arbitrarily (independently) selected for input into the formulation for the general case are ratio of specific heats, γ, Mach number, M_u, two of the three angles, μ, ν, and χ, cascade parameters S, h, and either phase angle, σ, or frequency, ω_u, along with distorton parameters L/p, q, and either amplitudes a and A or $\mathscr{a}$ and $\mathscr{A}$. Certain combinations of these parameters give a very orderly upstream distortion (vortical) motion which in turn, through the blade surface boundary condition, results in an especially clean acoustic motion upstream of the shock. Numerical results based on such flows are relatively easy to interpret and should aid in the analysis of more general cases which are within the capability of the theory.

As in Fig. 2 let $\nu = 0$ and $-\mu = \chi =$ wave angle given by $\sin^{-1}(1/M_u)$. Then $-\cot\mu = \beta_u = s/s^\dagger$. Let one transverse wave length fit the distance $\beta_u s$ along x and let $s^\dagger = N\beta_u s$ for integer N. Then $\beta_u^2 = 1/N$ and $M_u = (1 + 1/N)^{1/2}$. This wave pattern has a negative phase along $\Delta y = s$ which offsets the phase of the cycle along $\Delta x = \beta_u s$, leaving $\sigma = 2\pi(N - 1)$. Using (3) along with $d = 1/S = s^\dagger(1 + \cot^2\mu)$ it follows that $\omega_u = 2\pi(N - 1)S(1 + \cot^2\mu)/(1 - \cot^2\mu)$. The lowest N which clearly permits a subsonic mean axial velocity has a value of 2. For $N = 2$, $\sigma = 2\pi$, $M_u = (3/2)^{1/2}$, and $\chi = -\mu = \tan^{-1}\sqrt{2}$. Selecting a solidity of 1.3 then gives $\omega_u = 20.0$ (which is the passing frequency) and circumferential wave length $L/p = d = 0.769$. Amplitude ratio A/a is set equal to 0. Amplitude ratio C/a is then equal to $-4.7\, i/k_q$ by (4c). These results, along with $\gamma = 7/5$ and $k_q = \pi/3$ will be used as the basic reference condition for the numerical results herein.

Influence of Distortion on Blades Pressure Distribution

Pressure distribution along the upper and lower surfaces of the blades is given on Fig. 3(a) at the basic ordered condition. The short dashed line in the supersonic region represents a single airfoil solution [10]. Consistent with the reference cascade conditions on Fig. 2, the input to the airfoil theory is a transverse distortion having a wave length equal to $s^\dagger/2$. The resulting pressure distribution is normalized to match that of the cascade solution at the leading edge. The short wave length (high frequency) of the Bessel function solution of the airfoil is characteristic of the cascade solution also.[2] In the cascade this short wave length characteristic is carried a short distance downstream of the shock. The periodicity relation, $\phi(x,y) = e^{-ic}\,\phi(x + s^\dagger, y + s)$, is used in (22) to relate pressure on the lower surface of blade 1 to the upper surface of blade 0.

A second cascade solution (not shown) for a distortion with a phase angle of $\pi/2$ with respect to that of Fig. 3(a) is obtained from $\mathrm{Im}\left[p\, e^{i\omega_u t}/a \cos(k_q z)\right]$. This has the same wavelength characteristics and in the supersonic region agrees with single airfoil theory. Consistent with shock curvature and displacement, the pressure perturbation amplitude increased for the imaginary part, but decreased for the real part of the solution across this boundary for the reference conditions of Fig. 3(a).

The solution for Fig. 3(b) is based on the same set of parameters (for the ordered vortical motion) as Fig. 3(a) except σ, and therefore ω_u by (3), are reduced from the basic reference conditions by a factor of 1/8. Single airfoil theory is no longer close to these results and has been omitted. Trends are quite smooth and, of course, much more gradual than those of Fig. 3(a).

At very low interblade phase angles, $\sigma < \mathcal{O}(0.01)$, the pressure profile (not shown) across the channel is quite uniform and the pressure amplitude in back of the shock on the upper surface approaches that on the lower surface near the leading edge.

Influence of Cascade on Distortion Profile

Figure 4 uses the same basic reference conditions as in Fig. 3(a). Envision Fig. 4 as a view of the x-y plane of a blade channel. Located in this plane by use of the solid symbols are the leading and trailing edges of blades 0 and 1 and two reference Mach waves. Also located at various x stations are y distributions of the real part of the solution for the three transverse components of velocity in $u_2 = v_2 + w_2$. Far upstream of the cascade the amplitude of the acoustic motion (given by the short dashed line) goes to zero, however the vortical motion (long dashed line) is transported undiminished as if frozen in the flow. In the vicinity of the cascade the acoustic motion with its characteristic short wave length, due to diffraction about the leading edges, becomes quite prominent. Once inside the leading edge Mach wave of the nearest blade (blade 0) the transverse component of the acoustic velocity, $w_2^{(u)}$, is noticeably large only in the vicinity of the blade surface. The amplitude of the total motion, $u_2^{(u)}$, away from the wall is then mainly comprised of the relatively long wave length vortical motion, $v_2^{(u)}$. At x locations between the trailing edges of blades 0 and 1 the amplitude of the acoustic motion again becomes quite prominent, where diffraction in again encountered to satify the Kutta condition. Eventually $w_2^{(d)}$ decreases at large x to the asymptotic value at the last station, $x = \infty$. The amplitude of the vortical motion continues undiminished far downstream of the cascade and is not plotted at the last station.

The y distributions of $w_1^{(u)}$ has much the same nature as $w_2^{(u)}$. Although A, and therefore $v_1^{(u)}$, are zero, a longitudinal component of vorticity velocity, $v_1^{(d)}$, arises at the shock. Beyond this station both acoustic and vortical motions have trends with x much like those of $w_2^{(d)}$ and $v_2^{(d)}$. Recall that part of the vortical motion, $\bar{v}_d$ has been included in ϕ_d thus simplifying the wall boundary condition.

---

[2] Use of a reduced frequency of 20 thus permits comparison of two mathematical solutions to the linearized convected wave equation (6). It is possible that (6) may not offer a suitably accurate description of the motion, however, at such a high frequency. See, for example, chapter 1 of [11].

The y distribution of $w_3^{(u)}$ also follows a pattern somewhat similar to $w_4^{(u)}$. The influence of the shock on $v_3^{(d)}$ is small but quite pronounced on $w_3^{(d)}$ for the particular set of conditions of Fig. 4.

The z distributions of vortical and acoustic motions are not plotted since, by (2), (8), (19) and (39), they simply vary as $\cos(k_a z)$ for the transverse components of velocity and as $\sin(k_a z)$ for the spanwise components in both subsonic and supersonic regions.

Influence of Distortion and Cascade Parameters on Lift and Moment

Lift, $\mathcal{L}$, and moment, $\mathcal{M}$, were obtained by integration of the pressure distributions over the blade surfaces. Moments were taken about the center of the blade located at $x = 1/2 - s^\dagger$. Plots of the imaginary parts of lift and moment versus the corresponding real parts (chap. 9 of [12]) can be used to indicate the influence of various cascade and distortion parameters in stability studies. The contribution of shock movement to these terms can be obtained from plots as on Fig. 5(a). As in [2], the shocks are assumed to be attached to the lower surfaces of the blades (Fig. 1) arbitrarily near their leading edges. The allowed displacements, x_s, of the shock footprints on the upper blade surface, however, causes a lift $\mathcal{L}_s$, with amplitude equal to $(\bar{p}_d - \bar{p}_u)x_s$ within the confines of linearized theory. Here $\bar{p}_u$ and $\bar{p}_d$ are the steady pressures before and after the shock. This effect is included in the total lift and moment of Figs. 5(b) and (c). These figures are arbitrarily plotted at an interblade angle of 1/8 that of the reference set of conditions as in Fig. 3(b).

The variables h and a enter the equations for velocity potential (therefore for lift and moment) only as a/h and thus their influence can be expressed by spanwise wave number $k_a = \pi a/h$. This wave number should be most influential on amplitudes Φ_u and Φ_d when it is greater than k_u and k_d, respectively. This trend is illustrated in Fig. 5 by the large distance between tick marks on these curves at high k_a. Increase of upstream distortion amplitude ratio, A/a, tends to increase the magnitude of $\mathcal{L}$ and $\mathcal{M}$ at large k_a while preserving the spiral like k_a dependence. Cusps and/or loops characterize both the $\mathcal{L}_s$ and $\mathcal{L}$ curves. The magnitude of $\mathcal{L}_s$ is a significant part of $\mathcal{L}$.

CONCLUDING REMARKS

The influence of the third dimension on this analysis is primarily through the azimuthal wave number k_a. As k_a approaches zero the final equations and their solution reduce to much the same form as those of the flutter analysis of [2]. The main differences are in the boundary related terms where blade oscillation expressions of [2] are replaced by flow distortion expressions of the present study.

Selection of a combination of cascade and distortion parameters for a very orderly initial vortical motion gives in turn, through use of the blade surface boundary condition, an especially orderly acoustic motion as well. Numerical results based on such flows are relatively easy to interpret and aid in the analysis of more general cases which are within the capability of the theory. At these special conditions the supersonic pressure distribution reduces to shapes predicted by single airfoil theory. At high solidity the periodic pattern of the downstream running waves in the subsonic region of the cascade is quite evident in the blade pressure distribution. Influence of the reflected, or forward running, waves is mostly confined to within a relatively small distance of the trailing edges on the upper surfaces but is apparent over the distance $1 - 2s^\dagger < x \leq 1 - s^\dagger$ on the lower surfaces.

The strong in-passage shock has a large effect on lift and moment. Numerical results show large influences of interblade phase angle and therefore reduced frequency, longitudinal as well as transverse distortion amplitude, and azimuthal wave number on total as well as shock induced lift and moment. This suggests that any one of these distortion parameters could have considerable influence on the forced vibration effect in a stability analysis.

APPENDIX I

SOLUTION FOR ACOUSTIC MOTION UPSTREAM OF SHOCK

Substitution of (7) into (6) gives

$$\left[-\beta_u^2 \frac{\partial^2}{\partial x^2} + \frac{\partial^2}{\partial y^2} + 2iM_u k_u \beta_u^2 \frac{\partial}{\partial x} + \left(\beta_u^4 k_u^2 - k_a^2\right)\right]\Phi_u = 0. \tag{36}$$

A solution by separation of variables is $\exp\{-i[\alpha - M_u k_u)x + \beta_u \gamma_u y]\}$ where α is an arbitrary constant and $\gamma_u = \left(\alpha^2 - k_u^2 - k_a^2/\beta_u^2\right)^{1/2}$. Multiplying this result by $f(\alpha)\exp[-i(\alpha - M_u k_u)s^\dagger]$ and integrating over admissable values of α is also a solution of the linear homogeneous Eq. (10), where $f(\alpha)$ is yet to be determined.

Next, following the procedure of Lane and Friedman [4], apply this result to each of n blades using the local coordinate system $x_n = x - ns^\dagger$, $y_n = y - ns$ and specify that $f_n(\alpha)$ must satisfy the periodicity condition [5]

$$f_n(\alpha) = e^{in\sigma} f_0(\alpha) \tag{37}$$

for $n = 0, \pm 1, \pm 2, \cdots$. A solution with jump conditions across the n^{th} blade in proper form is then

$$\Phi_{u,n}(x_n, y_n) = \frac{\operatorname{sgn} y_n}{2\pi} \times \int_{-\infty+i\varepsilon}^{\infty+i\varepsilon} f_n(\alpha) e^{-i(\alpha - M_u k_u)s^\dagger} e^{-i[(\alpha - M_u k_u)x_n + \beta_u \gamma_u |y_n|]} d\alpha \tag{38}$$

where $\operatorname{sgn} y = \pm 1$ for $y \gtrless 0$. The branch points for γ_u are set at $\pm(\psi_u + i\varepsilon_u)$ where $\psi_u^2 = k_u^2 + k_a^2/\beta_u^2$ and ε_u is a small damping term. Now, as in [2], let $\varepsilon = M_u \varepsilon_u$ and $\operatorname{Im} k_u = \varepsilon_u$, then along the integration contour of (38) $\operatorname{Im}(\alpha - M_u k_u) = 0$, $\operatorname{Im} \gamma_u > 0$, and $|\exp\{i[(\alpha - M_u k_u)ns^\dagger + \beta_u \gamma_u |y_n|]\}| < 1$. Summing the

contribution of each blade to the potential yields a geometric series which can be expressed in closed form as

$$\phi_u(x,y) = \sum_{n=-\infty}^{\infty} \phi_{u,n}(x_n,y_n)$$

$$= \frac{1}{2\pi} \int_{-\omega+i\epsilon_u M_u}^{\omega+i\epsilon_u M_u} f_0(\alpha) A_u(\alpha,y) e^{-i(\alpha-M_u k_u)(x+s^+)} \, d\alpha \tag{39}$$

where

$$A_u(\alpha,y) \equiv \frac{1}{2i} \left[\frac{e^{i\left(\Delta_u^- + \beta_u \gamma_u y\right)}}{\sin \Delta_u^-} + \frac{e^{i\left(\Delta_u^+ - \beta_u \gamma_u y\right)}}{\sin \Delta_u^+} \right] \text{for } 0 \le y \le s \tag{40}$$

and

$$\Delta_u^{\pm} \equiv \frac{1}{2} \left(\alpha - M_u k_u s^+ + \alpha s^+ \pm \beta_u \gamma_u s \right). \tag{41}$$

Applying the flow tangency relation (5) to the surface of the $n = 0$ blade yields

$$-w_2^{(u)} = \frac{\partial \phi_u}{\partial y} = \frac{1}{2\pi}$$

$$\times \int_{-\omega+i\epsilon_u M_u}^{\omega+i\epsilon_u M_u} f_0(\alpha) \kappa_u(\alpha,0) e^{-i(\alpha-M_u k_u)\tilde{x}_u} \, d\alpha = e^{i\omega_u \tilde{x}_u} \tag{42}$$

for $\tilde{x}_u \equiv x + s^+ > 0$ and where

$$\kappa_u(\alpha,0) \equiv \partial A_u / \partial y \Big|_{y=0}. \tag{43}$$

The potential of the irrotational field produced upstream of the cascade must be continuous across lines $y = ns$ extending forward of the leading edges of the blades. Applying this boundary condition to (38) at the zeroth blade yields

$$\frac{1}{2\pi} \int_{-\omega+i\epsilon_u M_u}^{\omega+i\epsilon_u M_u} f_0(\alpha) e^{-i(\alpha-M_u k_u)\tilde{x}_u} \, d\alpha = 0 \quad \text{for} \quad \tilde{x}_u < 0. \tag{44}$$

Equations (42) and (44) are in the form of the upwash and continuity expressions of Ref. [4]. They differ from those of [2] only by the presence of k_0/β_u^2 in γ_u and by the distortion pattern, $e^{i\omega_u \tilde{x}_u}$, replacing the flutter motion on the right side of (42). The integrals in both of these equations are in the form of inverse Fourier transforms forming a two-part boundary value problem which can be solved for $f_0(\alpha)$ by the Wiener-Hopf technique [6]. Utilizing unilateral Fourier transforms [7] over $\tilde{x}_u$, the two equations are combined and then factored and decomposed into parts which are analytic in respective half planes as in Appendix B of [2], have a common region of analaticity between them, and vanish at ∞. The solution is completed by use of Liouville's theorm giving

$$f_0(\alpha) = \frac{i\kappa_u^- \left(\frac{k_u}{M_u} - i\epsilon_0 \right)}{\left(\alpha - \frac{k_u}{M_u} + i\epsilon_0 \right) \kappa_u^+(\alpha)} \tag{45}$$

Here ϵ_0 is a damping term on the distortion to ensure convergence as $\tilde{x}_u \to \infty$ and can be set equal to zero upstream of the shock.

The solution for $f_0(\alpha)$ required that $\kappa_u(\alpha)$ could be factored as $\kappa_u(\alpha,0) = \kappa_u^+(\alpha)/\kappa_u^-(\alpha)$ where $\kappa_u^+(\alpha)$ and $\kappa_u^-(\alpha)$ are analytic and non-zero in the upper ($\mathrm{Im}\ \alpha > M_u \epsilon_u$) and lower ($\mathrm{Im}\ \alpha < M_u \epsilon_u$) half planes respectively. The factoring procedure of Appendix C of [2] yields the results

$$\kappa_u^-(\alpha) = e^{-i\alpha\left(s^+ - \beta_u s\right)/2} \prod_{n=-\infty}^{\infty} \left(1 - \alpha/\nu_n^+ \right), \tag{46}$$

and

$$\kappa_u^+(\alpha) = e^{-i\alpha\left(s^+ - \beta_u s\right)/2} \frac{\beta_u \gamma_u}{2} \sin(\beta_u \gamma_u s)$$

$$\times \left[\left(\frac{c_u^+}{2} \right)^2 \nu_0^+ \nu_0^- \prod_{\substack{n=-\infty \\ \neq 0}}^{\infty} \left(\frac{c_u^+}{2n\pi} \right)^2 \nu_n^+ \nu_n^- \right]^{-1} \left[\prod_{n=-\infty}^{\infty} \left(1 - \frac{\alpha}{\nu_n^-} \right) \right]^{-1}, \tag{47}$$

$$c_u^+ = \left(s^{+2} - \beta_u^2 s^2 \right)^{1/2}, \tag{48}$$

$$\nu_n^{\pm} = \Gamma_n^{(u)} \frac{s^+}{c_u^+} \pm \frac{\beta_u s}{c_u^+} \left[\left(\Gamma_n^{(u)} \right)^2 - k_u^2 - \frac{k_0^2}{\beta_u^2} \right]^{1/2}, \tag{49}$$

$$\Gamma_n^{(u)} = \left(2n\pi + M_u k_u s^+ - \alpha \right) / c_u^+. \tag{50}$$

Equations (46) through (50) differ from those of Ref. [2] only by the presence of k_a in the definitions of γ_u and $\nu_n^{\pm}$.

Substitution of (45) into (39) enables determination of $\phi_u(x,y)$ by the method of residues. The path of integration is closed in the upper half-plane for $x < -\beta_u(s - y)$ and in the lower half-plane for $x > -\beta_u(s - y)$.

APPENDIX II

SOLUTION FOR ACOUSTIC MOTION DOWNSTREAM OF SHOCK

An infinite "duct" solution to the convected wave equation for downstream running waves can be obtained by use of the method of separation of variables. This gives the result

$$\phi_d^{duct}(x,y) = \frac{1}{\pi}\sum_{n=0}^{\infty} B_n \frac{e^{in_n^+ \tilde{x}_d}\cos(n\pi y/s)}{\frac{k_d}{M_d} - \lambda_n^{(d)}}, \qquad (51)$$

where

$$n_n^{\pm} = -M_d k_d \pm \lambda_n^{(d)}, \qquad (52)$$

and

$$\lambda_n^{(d)} = i\left[(n\pi/\beta_c s)^2 - k_d^2 + k_a^2/\beta_c^2\right]^{1/2} \qquad (53)$$

By chapter 5 of [3] the cascade potential for upstream running waves can be expressed as

$$\phi_d^{cascade}(x,y) = \frac{1}{2\pi}\int_{-\infty}^{\infty} \frac{f_0(\alpha)A_d(\alpha,y)}{\alpha + k_d/M_d} e^{-i(\alpha+M_d k_d)\tilde{x}_d}\, d\alpha \qquad (54)$$

where, in slightly different nomenclature than [3]

$$A_d = \frac{1}{2i}\left[\frac{e^{i\Delta_d^+ - \beta_d\gamma_d y}}{\sin\Delta_d^+} + \frac{e^{i\Delta_d^- + \beta_d\gamma_d y}}{\sin\Delta_d^-}\right] \qquad (55)$$

$$\Delta_d^{\pm} = \frac{1}{2}\left(\alpha + M_d k_c s^+ + \alpha s^+\right) \pm \beta_d\gamma_d s/2i \qquad (56)$$

$$\gamma_c = \left(\alpha^2 - k_d^2 + k_a^2/\beta_c^2\right)^{1/2} \qquad (57)$$

For this linear problem, where superposition applies, let

$$f_0 = \frac{1}{\pi}\sum_{n=0}^{\infty} B_n f_{0,n}(\alpha) \qquad (58)$$

By (54) and (58) the zero upwash condition will be satisfied if

$$\int_{-\infty}^{\infty} f_{0,n}(\alpha)\kappa_d(\alpha,0)e^{-i(\alpha-M_d k_d)\tilde{x}_d}\, d\alpha = 0 \quad \text{for} \quad \tilde{x}_d < 0 \qquad (59)$$

where

$$\kappa_d(\alpha,C) \equiv -\partial\Lambda_d/\partial y\Big|_{y=0}(\alpha + k_d/M_d)^{-1} \qquad (60)$$

A relation specifying zero pressure jump across lines extending in the downstream direction from the trailing edges of the blades is obtained by substituting (51) and (54) through (58) into $P_d = (i\omega_d - \partial/\partial x)(\phi_d^{duct} + \phi_d^{cascade})$ and utilizing the periodicity relation. The resulting expression can be reduced to

$$\int_{-\infty}^{\infty} f_{0,n}(\alpha)e^{-i\alpha\tilde{x}_d}\, d\alpha = e^{i\left(n_n^+ + M_d k_d\right)\tilde{x}_d}\left[e^{i\left(n_n^+ s^+ - \sigma + n\pi\right)} - 1\right] \quad \text{for} \quad \tilde{x}_d > 0 \qquad (61)$$

Solution of Eqs. (59) and (61) again constitutes a Wiener-Hopf problem which can be solved in much the same manner as in the supersonic case yielding

$$f_{0,n}(\alpha) = \frac{\kappa_c^-\left(-\lambda_n^{(d)}\right)}{2i\left(\alpha + \lambda_n^{(d)}\right)\kappa_c^-(\alpha)}\left[1 - e^{i\left(n_n^+ s^+ - \sigma + n\pi\right)}\right] \qquad (62)$$

Here it is assumed that κ_d can be factored into the form $\kappa_d^-(\alpha)/\kappa_d^+(\alpha)$ where $\kappa_d^+(\alpha)$ and $\kappa_d^-(\alpha)$ are analytic and non-zero in upper and lower half planes respectively. To perform this factorization substitute (55) into (60) and obtain

$$(\alpha + k_d/M_d)\kappa_d(\alpha,0) = \beta_d\gamma_d \sinh(\beta_d\gamma_d s)\Big/\left(2\sin\Delta_d^+\sin\Delta_d^-\right) \qquad (63)$$

The numerator of (63) can be factored by the Weierstrass factorization formula [7]. Page 40 of [6] is helpful for application of this theorem to the denominator. Choose the half planes as in Fig. 8 of [2] but with branch points of γ_d at $\pm(\psi_d + i\epsilon_d)$ where $\psi_d = k_d - k_a/\beta_d$. Then

$$\kappa_d^-(\alpha) = \frac{(\alpha - \psi_d)\sin(\beta_d\psi_d s)e^{i\alpha b/\pi}}{\psi_d\left[\cos(\beta_d\psi_d s) - \cos\left(\sigma - M_d k_d s^\dagger\right)\right]\left(1 - \alpha/\alpha_0^+\right)}$$

$$\times \prod_{n=1}^{\infty} \frac{1 - \alpha/\lambda_n^{(d)}}{\left(1 - \alpha/\alpha_n^+\right)\left(1 - \alpha/\alpha_{-n}^+\right)} \qquad (64)$$

and

$$\kappa_d^+(\alpha) = \frac{(\alpha + k_d/M_d)\left(1 - \alpha/\alpha_0^-\right)e^{i\alpha b/\pi}}{\beta_d(\alpha + \psi_d)}$$

$$\times \prod_{n=1}^{\infty} \frac{\left(1 - \alpha/\alpha_n^-\right)\left(1 - \alpha/\alpha_{-n}^-\right)}{1 + \alpha/\lambda_n^{(c)}} \qquad (65)$$

where

$$h \equiv s^\dagger\left[\frac{1}{2}\pi - \tan^{-1}\left(s\beta_d/s^\dagger\right)\right] + s\beta_c \ln\left(2s\beta_c/d_c^\dagger\right), \qquad (66)$$

$$\Gamma_n^{(d)} \equiv \left(2n\pi - \sigma - M_d k_c s^\dagger\right)/d_c^\dagger, \qquad (67)$$

$$c_c^\dagger \equiv \left(s^{\dagger 2} + \beta_c^2 s^2\right)^{1/2}, \qquad (68)$$

$$\alpha_n^\pm \equiv \Gamma_n^{(d)}\frac{s^\dagger}{c_c^\dagger} \pm i\frac{\beta_d s}{c_c^\dagger}\left[\left(\Gamma_n^{(d)}\right)^2 - k_d^2 + \frac{k_0^2}{\beta_d^2}\right]^{1/2}, \qquad (69)$$

and ψ_d in equal to $\left|k_c^2 - k_0^2/\beta_d^2\right|^{1/2}$ and $i\left|k_0^2/\beta_c^2 - k_d^2\right|^{1/2}$ for k_c^2 greater than and less than k_0^2/β_c^2 respectively. Equations (64) through (69) reduce to those of Appendix E of [2] as $k_0 \to 0$. Substitution of (62) and (55) through (58) into (54) gives an integral expression for $\phi_d^{cascade}$ which can be evaluated by use of the residue theorm. The integrand of (54) can be expressed as $I = I_1 - I_2$ where the α dependence enters I_1 as

$$\cosh\left[\beta_c\alpha(y - s)\right]\Big/\left[\beta_c\alpha^2\kappa_c^+(\alpha)\sinh(\beta_c\alpha s)\exp(i\alpha\tilde{x}_c)\right]$$

as $\alpha \to \infty$

and I_2 as

$$\cosh\left[\beta_c\alpha y\right]\Big/\left\{\beta_c\alpha^2\kappa_d^+(\alpha)\sinh(\beta_c\alpha s)\exp\left[i\alpha\left(\tilde{x}_d - s^\dagger\right)\right]\right\}$$

as $\alpha \to \infty$.

For I_1 the path of integration must be closed in the upper half plane (UHP) for $\tilde{x}_c < 0$ and LHP for $\tilde{x}_d > 0$. The path for I_2 must be closed in UHP for $\tilde{x}_d < s^\dagger$ and LHP for $\tilde{x}_d > s^\dagger$. Finally, the total amplitude, ϕ_d, for $0 \le y \le s$ is obtained by combining ϕ_d^{duct} with $\phi_d^{cascade}$.

REFERENCES

1. Fleeter, S., "Aeroelasticity Research for Turbomachine Applications," Journal of Aircraft, Vol. 16, No. 5, May 1979, pp. 320-326.
2. Goldstein, M. E., Braun, W., and Adamczyk, J. J., "Unsteady Flow in a Supersonic Cascade with Strong In-Passage Shocks," Journal of Fluid Mechanics, Vol. 83, part 3, Dec. 1977, pp. 569-604.
3. Goldstein, M. E., Aeroacoustics, McGraw-Hill, New York, 1976.
4. Lane, F., and Friedman, M., "Theoretical Investigation of Subsonic Oscillatory Blade-Row Aerodynamics," NACA TN-4136, 1958.
5. Lane, F., "System Mode Shapes in the Flutter of Compressor Blade Rows," Journal of Aeronautical Science, Vol. 23, No. 1, Jan. 1956, pp. 54-66.
6. Noble, B., Methods Based on the Wiener-Hopf Technique for the Solution of Partial Differential Equations, Pergamon Press, New York, 1958.
7. Roos, B. W., Analytic Functions and Distributions in Physics and Engineering, John Wiley, New York, 1969.
8. Moore, F. K., "Unsteady Oblique Interaction of a Shock Wave with a Plane Disturbance," NACA TR-1165, 1954.
9. Peirce, B. O., A Short Table of Integrals, 3rd rev. ed., Ginn and Co., Boston, 1929.
10. Kaji, S., "Noncompact Source Effect on the Prediction of Tone Noise from a Fan Rotor," Aeroacoustics: Fan Noise and Control; Duct Acoustics; Rotor Noise, I. R. Schwartz, H. T. Nagamatsu and W. C. Strahle, eds., Progress in Astronautics and Aeronautics, Vol. 44, American Institute of Aeronautics and Astronautics, New York, 1976, pp. 55-81.
11. Miles, J. W., The Potential Theory of Unsteady Supersonic Flow, Cambridge, University Press, 1959.
12. Bisplinghoff, R. L., Ashley, H., and Halfman, R. L., Aeroelasticity, Addison-Wesley, Cambridge, MA, 1955.

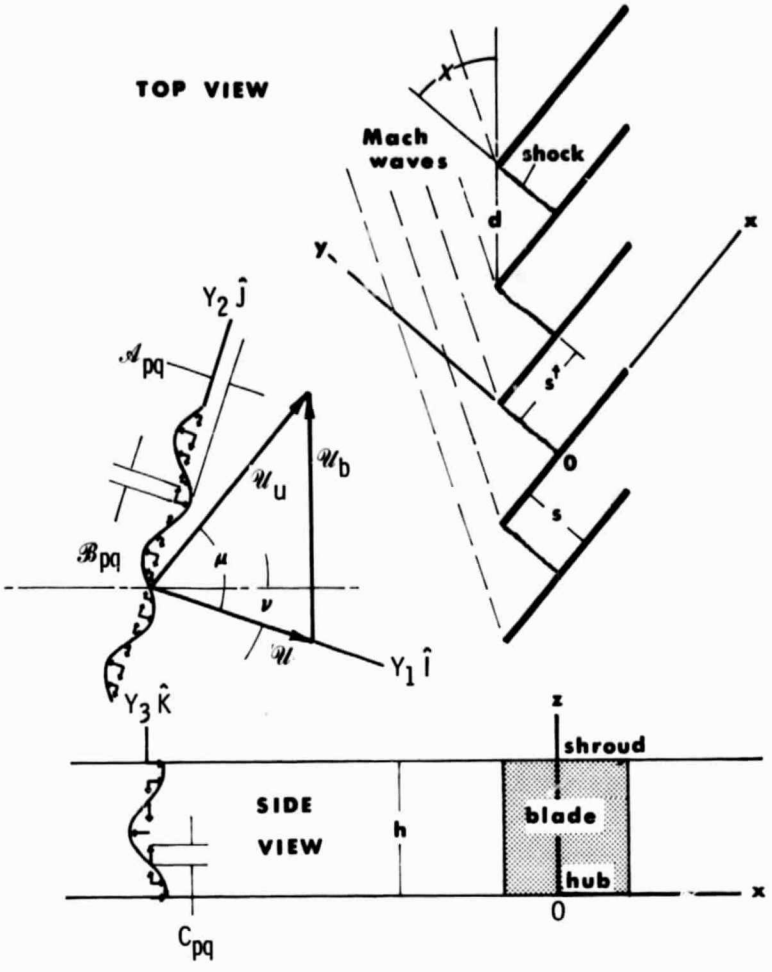

Figure 1. - Orientation of upstream distortion with respect to cascade.

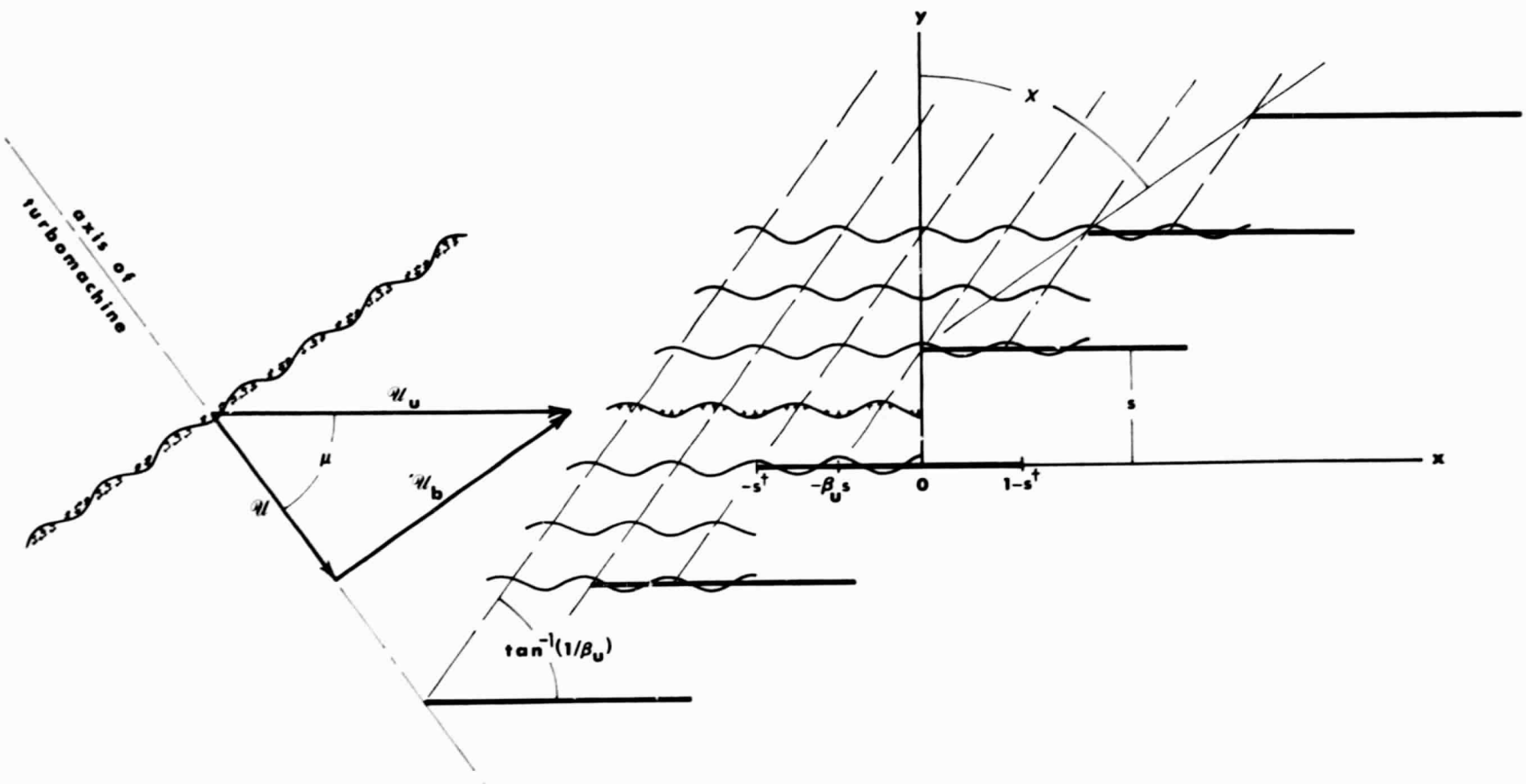

Figure 2. - Select distortion (vortical) pattern of v_2 entering blade channels for use as a reference condition: $N = 2$, $\sigma = 2\pi$, $M_U = (3/2)^{1/2}$, $\chi = -\mu = \tan^{-1}(2)^{1/2}$, and $A = 0$.

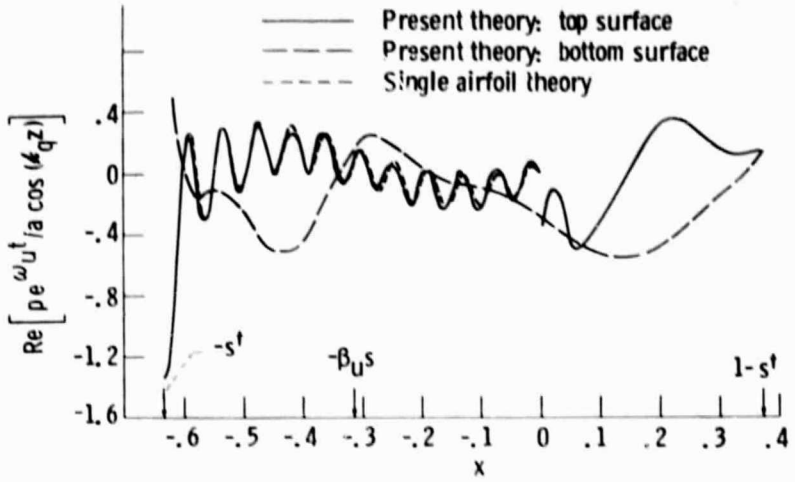

(a) Distortion and cascade at basic reference conditions of Figure 2 along with S = 1.3, ω_U = 20.0, and $k_Q = \pi/3$.

Figure 3. - Pressure distribution on zeroth blade.

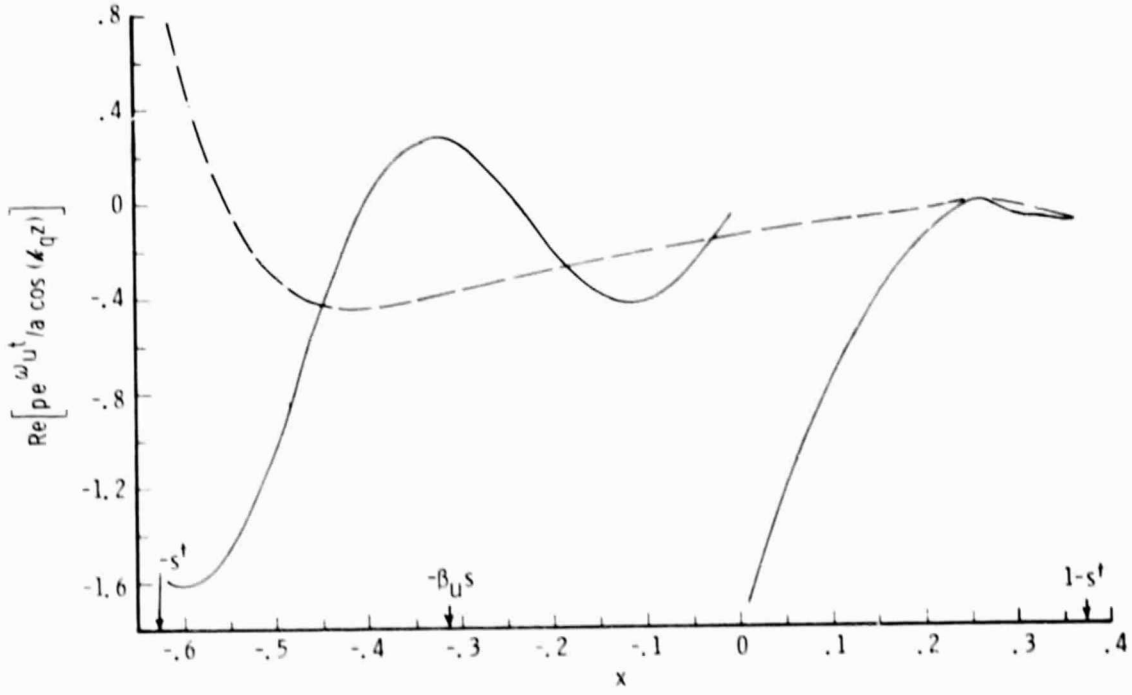

(b) Distortion and cascade conditions same as Figure 3(a), except that σ and ω_U are reduced to $2\pi/8$ and 20.0/8, respectively

Figure 3. - Concluded.

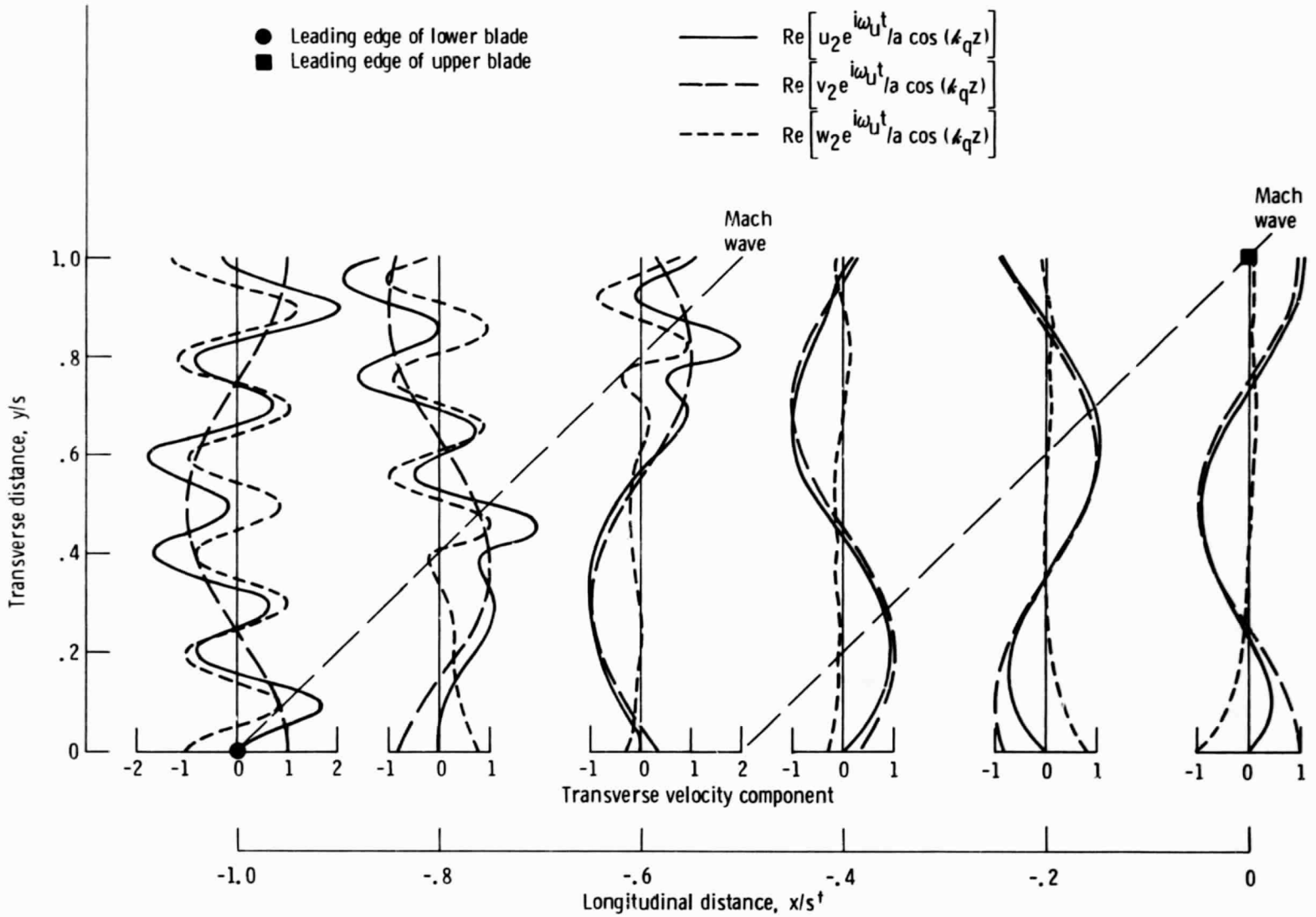

(a) Upstream of shock.

Figure 4. - Channel-wise distribution of y components of velocity at various longitudinal locations along blade. Distortion and cascade conditions same as in Figure 3.

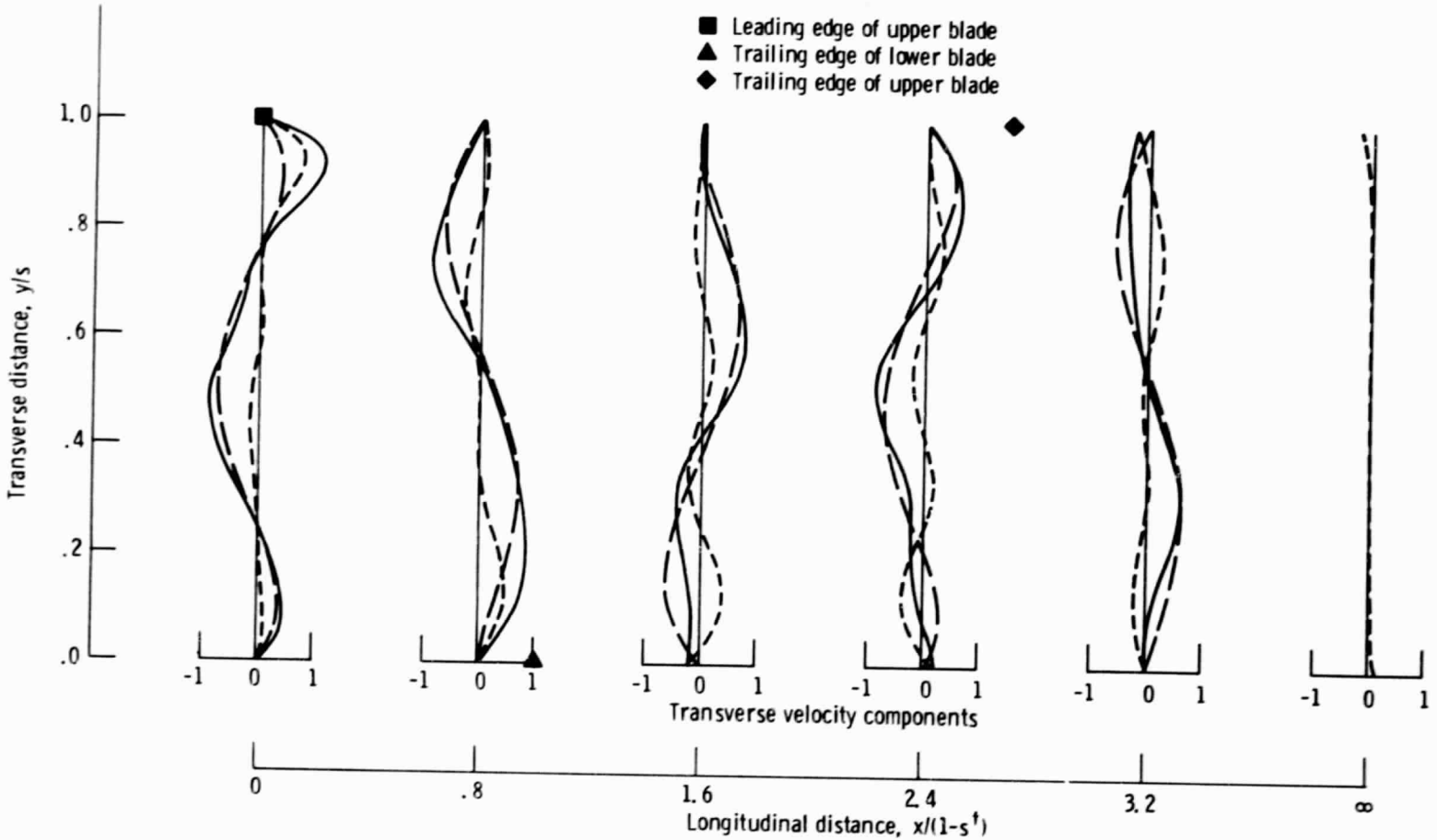

(b) Downstream of shock.

Figure 4. - Concluded.

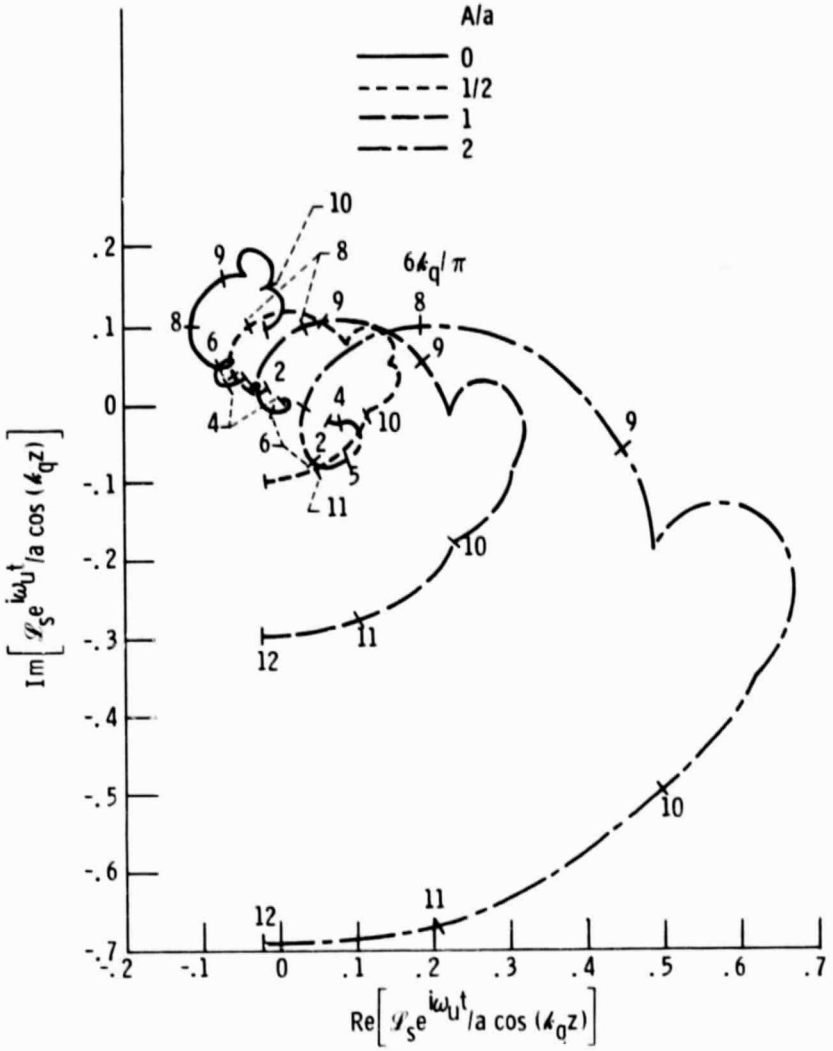

(a) Shock induced lift, $\mathscr{L}_s$.

Figure 5. - Influence of azimuthal wave number, k_q, and distortion amplitude ratio, A/a, on lift and moment.

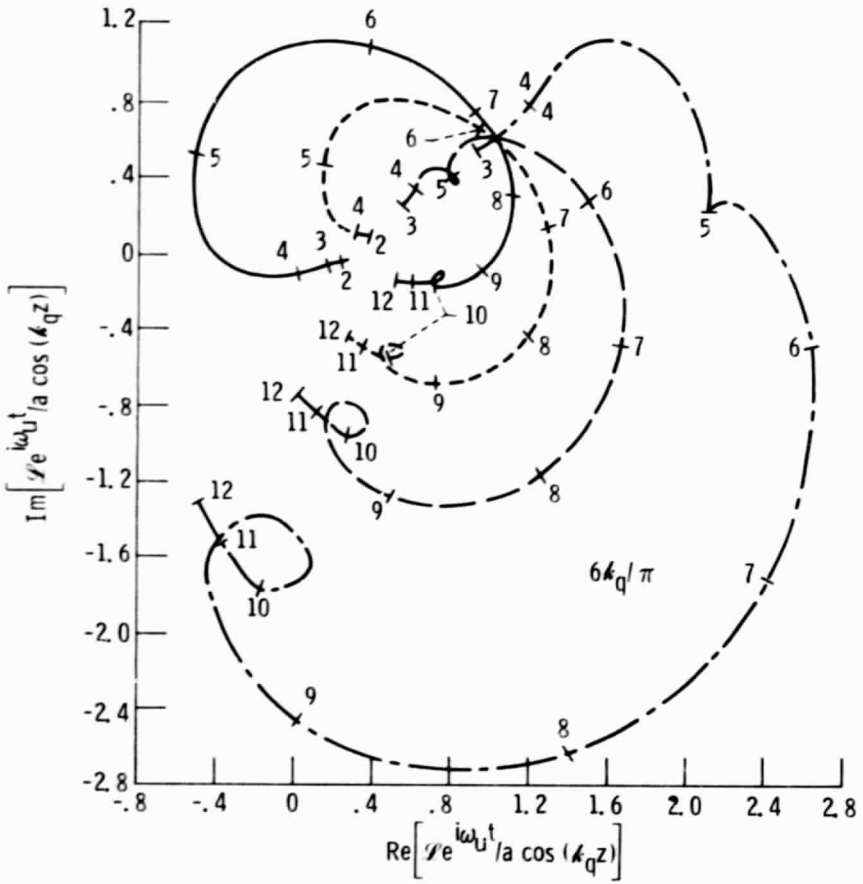

(b) Total lift, $\mathscr{Y}$.

Figure 5. - Continued.

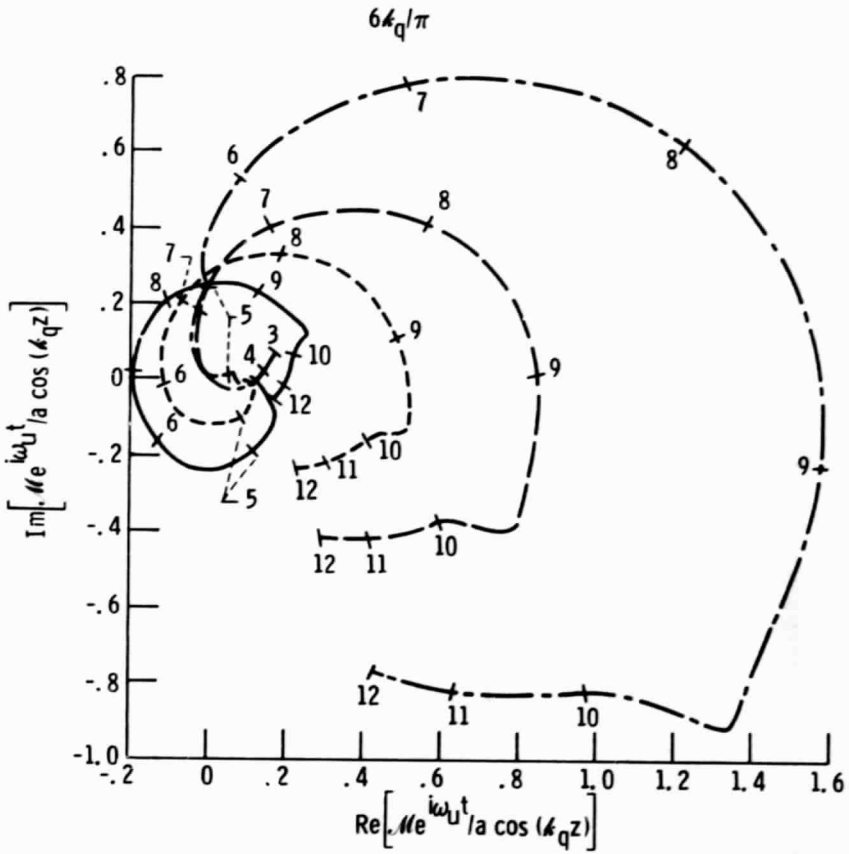

(c) Moment, $\mathscr{M}$.

Figure 5. - Concluded.